AD_____

Award Number: DAMD17-00-1-0168

TITLE: Differential Expression of DNA Double-Strand Break Repair Proteins in Breast Cells

PRINCIPAL INVESTIGATOR: Carl W. Anderson, Ph.D.
Mangala Tawde, Ph.D.

CONTRACTING ORGANIZATION: Brookhaven National Laboratory
Upton, New York 11973-5000

REPORT DATE: July 2002

TYPE OF REPORT: Annual

PREPARED FOR: U.S. Army Medical Research and Materiel Command
Fort Detrick, Maryland 21702-5012

# REPORT DOCUMENTATION PAGE

*Form Approved*
*OMB No. 074-0188*



| 1. AGENCY USE ONLY (Leave blank) | 2. REPORT DATE | 3. REPORT TYPE AND DATES COVERED |
|---|---|---|
| | July 2002 | Annual (1 Jul 01 - 30 Jun 02) |

**4. TITLE AND SUBTITLE**
Differential Expression of DNA Double-Strand Break Repair Proteins in Breast Cells

**5. FUNDING NUMBERS**
DAMD17-00-1-0168

**6. AUTHOR(S)**
Carl W. Anderson, Ph.D.
Mangala Tawde, Ph.D.

**7. PERFORMING ORGANIZATION NAME(S) AND ADDRESS(ES)**
Brookhaven National Laboratory
Upton, New York 11973-5000

E-Mail: cwa@bnl.gov

**8. PERFORMING ORGANIZATION REPORT NUMBER**

**9. SPONSORING / MONITORING AGENCY NAME(S) AND ADDRESS(ES)**
U.S. Army Medical Research and Materiel Command
Fort Detrick, Maryland 21702-5012

**10. SPONSORING / MONITORING AGENCY REPORT NUMBER**



**11. SUPPLEMENTARY NOTES**
report contains color

**12a. DISTRIBUTION / AVAILABILITY STATEMENT**
Approved for Public Release; Distribution Unlimited

**12b. DISTRIBUTION CODE**

**13. Abstract** ***(Maximum 200 Words)*** *(abstract should contain no proprietary or confidential information)*
Two mechanisms that repair DNA double-strand breaks in mammalian cells are homologous recombination and non-homologous DNA end-joining (NHEJ). Previous studies showed that a critical component of the NHEJ pathway, the DNA-activated protein kinase (DNA-PK), was poorly expressed in non-lactating (resting) breast tissue. Therefore, we proposed to identify the mechanisms responsible for regulating levels of non-homologous end-joining DNA repair components in human breast tissue and to measure the DNA double-strand break repair capacity of breast epithelial cells.

We reexamined the expression of DNA-PK in human breast tissues by immuno-histochemistry and extended these studies to two other components of the NHEJ repair pathway, XRCC4 and DNA ligase IV, as well as other DNA repair components including NBS1 and MRE11. In contrast to the original report, 90% of the epithelial cells in normal resting breast tissues from 10 different patients expressed both components of DNA-PK, DNAPKcs and Ku. In contrast, stromal cells failed to express NHEJ proteins, but a cell line derived from breast stromal tissue did. No polymorphisms were detected in the Ku70 gene of 14 breast cancer patients, but 11.3% of breast cancer patients amplified the gene for the Wip1 phosphatase that regulates p53 activity.

| 14. SUBJECT TERMS | 15. NUMBER OF PAGES |
|---|---|
| gene expression, epithelial cells, cell differentiation, DNA repair | 22 |
| | 16. PRICE CODE |

| 17. SECURITY CLASSIFICATION OF REPORT | 18. SECURITY CLASSIFICATION OF THIS PAGE | 19. SECURITY CLASSIFICATION OF ABSTRACT | 20. LIMITATION OF ABSTRACT |
|---|---|---|---|
| Unclassified | Unclassified | Unclassified | Unlimited |

# Table of Contents

## Introduction

DNA double-strand break (DSB) repair is critical for cell survival and for preventing genome rearrangements leading to cancer. It is carried out by two mechanisms, homologous recombination and non-homologous DNA end joining (NHEJ). NHEJ is the major repair pathway of DNA repair in mammalian cells and is mediated by three complexes: the DNA-PK complex (DNA-PKcs, Ku70, Ku80), the XRCC4/DNA Ligase IV complex and the NBS1/Rad50/MRE11 complex. We recently observed that DNA-activated protein kinase (DNA-PKcs), a critical component of the NHEJ repair pathway in vertebrates, was poorly expressed in non-lactating (resting) human breast tissue compared to lactating breast tissue, where it was expressed at high levels. All tissues exhibited similar amounts of mRNAs for the three polypeptide components that comprise DNA-PK, suggesting that the poor expression of DNA-PKcs in resting breast epithelial cells results from posttranscriptional mechanisms rather than transcriptional regulation. Our findings suggested that resting breast tissue might be compromised for the repair of DSBs compared to other tissues. Therefore we proposed to measure the DNA double-strand break repair capacity of breast cells and identify the mechanisms responsible for regulating levels of NHEJ DNA repair components in human breast tissue.

To accomplish these goals, we proposed to: I) establish culture conditions that recapitulate DNA-PK and NHEJ component expression in breast tissue; II) examine the effects of low and high expression levels on DNA repair and genome stability; III) identify the mechanisms that regulate NHEJ component expression in breast tissue.

## Body

The objectives of this project were based on the findings (Moll et al., 1999) that epithelial cells in lactating human breast tissue expressed high levels of both DNA-PKcs and Ku proteins while none of these proteins were detected in epithelial cells in normal (resting) human breast tissue. However (as stated in last annual report), when these findings were recapitulated on a larger scale, both resting as well as lactating breast tissue sections of normal women showed strong expression of DNA-PKcs, Ku70, Ku80, XRCC4, and DNA ligase IV as well as NBS1 and MRE11. The interesting observation emerging from our analysis was that stromal cells in these breast tissue sections were devoid of any of these proteins or expressed them at very low levels. Micrographs of breast tissue sections stained with antibodies to DNA-PKcs and other DNA repair proteins are shown in Figure 1.

To investigate the expression of NHEJ proteins in stromal cells from breast tissue in more detail, a representative stromal cell line was identified and obtained from ATCC (cat. # CRL-7345). This cell line, Hs 574.T, which is of fibroblast type, was derived from the ductal carcinoma of human mammary gland and apparently is of stromal origin. The cell line is from the Naval Biosciences Laboratory collection that was transferred to the ATTC in 1982.

Expression of DNA-PKcs and other NHEJ repair proteins has been studied in Hs 574.T cells by immunocytochemistry and Western immunoblot assay using available antibodies specific for each NHEJ protein. The expression of DNA-PKcs and both Ku proteins were found to be comparable to expression in other human cell lines including HeLa and MO59K (Figure 2). The DNA-PK activity in these cells was assayed and also was found to be comparable to that in other human cell lines (Figure 3). These data suggest that, although stromal cells are negative in DNA-PKcs expression *in vivo*, they acquire a DNA-PKcs positive phenotype when grown in culture. This result is consistent with the observation that proliferating cells show higher levels of DNA-PKcs than resting cells (Kubota et al., 1998; Erikson et al., 2000) and that stromal cells *in vivo* are terminally differentiated (non-dividing). To determine if the corollary is true *in vivo*, that is if DNA-PKcs is low in resting, terminally differentiated breast tissue, we propose to analyze the epithelial as well as the stromal cells in breast tissue sections from post-menopausal (vs. pre-menopausal) women where the major part of this gland should be at rest and in a non-proliferating state, i.e. the cells are terminally differentiated and have stopped dividing.

Okayasu et al. (2000) reported that DNA-PKcs and the Ku proteins were expressed at lower levels in mouse breast tissues than in other mouse tissues. They further showed that BALB/c mice, which are 20 times more susceptible to low-level radiation-induced breast cancer than most other mouse strains (e.g. C57Black), expressed less DNA-PKcs protein than radiation resistant mouse strains; however, Ku70 and Ku80 expression was similar in both sensitive and resistant strains. Furthermore, breast cancer susceptibility was associated with DNA double-strand break repair capacity, radiosensitivity and DNA-PKcs expression. More recently, two differences in the amino acid sequence of DNA-PKcs from BALB/c mice compared to C57Black mice were discovered (Yu et al., 2001). Although DNA-PK has been implicated in the cellular response to ionizing radiation in mammalian cells (Muller et al., 1999), no correlation has yet been observed between radiosensitivity in cancer patients and the expression and activities of DNA repair proteins in the fibroblast cell lines derived from these patients (Carlomagno et al., 2000). Nevertheless, it was reported that cell lines from more than 40 percent of human breast cancer patients exhibit increased genome instability (Scott et al., 1994). The absence of a correlation between NHEJ expression or activity could be a consequence of limitations of the detection techniques used in the studies (immunohistochemistry and western blot analysis); therefore, we propose to reexamine this issue by using more sensitive assays such as flow cytometric analysis (FACS) and quantitative immunohistocytochemistry (IHC). Depending on availability, FACS will be carried out on lymphocytes from patients with different radiosensitivities whereas quantitative IHC will be carried out on the paraffin-embedded tissue sections from these patients. Genomic instability studies also will be carried out on these patients.

The mouse studies described above suggest that polymorphisms in NHEJ genes may result in decreased repair of DNA double-strand breaks and increased cancer susceptibility through effects on protein expression, stability or specific activity. Through Dr. W. Kauffmann, Lineberger Cancer Center, University of North Carolina, DNAs from EBV immortalized lymphocytes derived from 14 breast cancer patients participating in the Carolina Breast Cancer Program were obtained. The lymphocytes from seven of these individuals exhibit a chromosome

breakage phenotype when exposed to ionizing radiation in the G2 phase of the cell cycle (see Scott et al., 1994), while the remaining seven do not. Using an ABI 3100 automated DNA sequencer, both strands of PCR segments corresponding to each of the thirteen exons of the Ku70 gene from these 14 individuals were sequenced. No polymorphisms were identified that altered the amino acid sequence of Ku70, indicating that polymorphisms in Ku70 are not responsible for the breast cancer-related radiation sensitivity phenotype. Similar analyses of the 21 exons of Ku80 and the 86 exons of DNA-PKcs are in progress.

Through other resources, antibody reagents for analyzing posttranslational modifications to the p53 tumor suppressor protein have been developed. Analysis of p53 from oncogenic Ras transformed human IMR-90 human normal lung fibroblasts demonstrated phosphorylation on Ser33 and Ser46, indicative of phosphorylation by p38 MAPK. Overexpression of Wip1, a p53 induced protein phosphatase that inactivates p38 MAPK, decreased p53 phosphorylation at Ser33 and Ser46 and partially reversed Ras-induced senescence. Analysis of 64 human tumor lines showed that the Wip1 gene, *PPM1D*, at 17q22/23 was amplified in several breast tumor cell lines. Thirty-seven of 326 primary breast tumors (11.3%) also exhibited *PPM1D* amplification, suggesting that p53 inactivation through *PPM1D* amplification and overexpression may contribute to the development of human breast cancer. These studies were reported in *Nature Genetics*.

## Key Research Accomplishments

- Rexamined expression of DNA-PKcs , Ku80 and other NHEJ components, including XRCC4, DNA ligase IV and NBS1/MRE11 in epithelial cells from resting human breast tissue; each protein was expressed at similar, readily detectable levels.
- Examined expression of NHEJ components in stromal cells from resting and lactating human breast tissue; none were expressed.
- Identified a human breast stromal cell line in which expression of DNA repair proteins could be examined to determine if reduced expression of NHEJ proteins is recapitulated.
- Studied expression of DNA-PKcs and Ku80 in cultured stromal cells as well as other human cell lines; expression was comparable to that found in other human cell lines.
- DNA-PK activity was assayed in cultured stromal cells, which also was found to be comparable to that found in other human cell lines.
- Showed no correlation between polymorphisms in Ku70 and radiation induced chromosome breakage phenotype.
- Determined an absence of polymorphisms in *KU70* from lymphocytes of breast cancer patients with and without a DNA breakage phenotype.
- Identified *PPM1D*, the gene for the Wip1 phosphatase, as a gene frequently amplified in breast cancer patients with wildtype *TP53*.

## Reportable Outcomes

- **Differential expression of DNA double-strand break repair proteins in human breast cells** - M. Tawde, P. Friemuth, C. Anderson. Abstract sent for poster presentation at the Era of Hope DoD Breast Cancer Research Program meeting being held at Orlando, FL on September 25-28, 2002.
- **Differential expression of DNA double-strand break repair proteins.** Manuscript in preparation.
- **Amplification of *PPM1D* in human tumors abrogates p53 tumor suppressor activity**. D.V. Bulavin, O.N. Demidov, S. Saito, P. Kauraniemi, C. Phillips, S.A. Amundson, C. Ambrosino, G. Sauter, A.R. Nebreda, C.W. Anderson, A. Kallioniemi, A.J. Fornace, Jr., and E. Appella. *Nat Genet* **31**: 210 (2002).

## Conclusions

Both resting as well as lactating breast tissue sections of normal women showed strong expression of DNA-PK, Ku70/80, XRCC-4, DNA Ligase IV as well as NBS1 and MRE11 in epithelial cells. The stromal cells in these tissue sections were found to be devoid of or to express low levels of each of these proteins. Although stromal cells in tissue sections showed low DNA-PK expression, when cultured *in vitro* they exhibited moderate expression levels and activity. Proliferating cells exhibit higher DNA-PK expression and activity compared with non-proliferating or resting cells.

## References


1. U. Moll, R. Lau, M. Sypes, M. Gupta, C. W. Anderson, *Oncogene* **18**, 3114 (1999).
2. R. Okayasu, K. Suetomi, Y. Yu, A. Silver, J. S. Bedford, R. Cox, R. L. Ullrich, *Cancer Res* **60**, 4342 (2000).
3. C. Muller, G. Rodrigo, P. Calsou, B. Salles, *Bull Cancer* **86**, 977 (1999).
4. F. Carlomagno, N. G. Burnet, I. Turesson, J. Nyman, J. H. Peacock, A. M. Dunning, B. A. Ponder, S. P. Jackson, *Int J Cancer* **85**, 845 (2000).
5. Y. Yu, R. Okayasu, M. M. Weil, A. Silver, M. McCarthy, R. Zabriskie, S. Long, R. Cox, R. L. Ullrich, *Cancer Res* **61**, 1820 (2001).
6. D. Scott, A. Spreadborough, E. Levine, S. A. Roberts, *Lancet* **344**, 1444 (1994).
7. Kubota N, Ozawa F, Okada S, Inada T, Komatsu K, Okayasu R, *Cancer Let* **133**, 161(1998).
8. A. Erikson, R. Lewensohn, A. Nilson, *Anticancer Res* **20**, 3051 (2000).
9. Y. Achari, S. P. Lees-Miller, *Methods Mol Biol*) **99**, 85 (1999).
10. N, J, Finnie, T. M. Gottlieb, T. Blunt, P. A. Jeggo, S. P. Jackson, *Proc Natl Acad Sci USA* **92**, 320 (1995).

# Appendix I

DAM17-00-1-0168
Carl W. Anderson

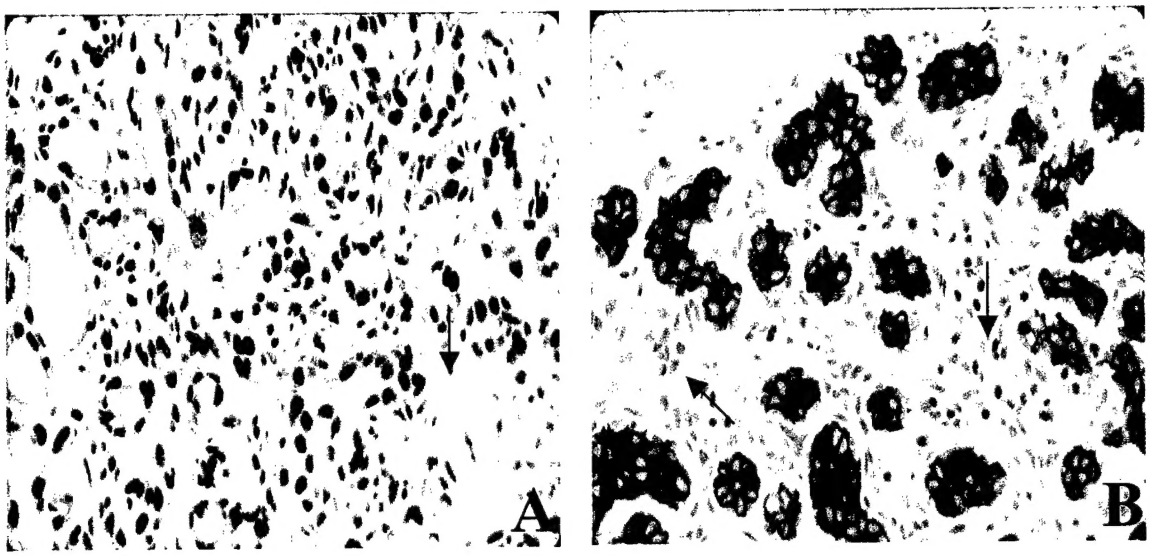


**Figure 1. Expression of NHEJ repair proteins in human breast tissue.** (A) DNA-PKcs and (B) Ku80 in resting breast tissue. Note that the stromal cells, indicated by arrows, are negative. Tissues came from the routine pathology archives of the department of Pathology, University Hospital at SUNY Stony Brook. After biopsy or resection, the tissues were fixed in 10% formalin for upto 18 h and processed for light microscopy by standard methods. Immunohistochemical staining was as described in Moll et al. (1999). Briefly, 4 μm paraffin sections were deparaffinized by microwaving sections in 100 mM citric acid buffer, pH 6.0 for 5 min, 6 times. Sections then were treated with 0.3% $H_2O_2$ / methanol to quench endogenous peroxidase activity. After blocking with 10% normal goat serum, sections were incubated at 4°C overnight with primary antibody in 2% bovine serum albumin/phosphate buffered saline. Biotinylated goat anti-mouse or goat anti-rabbit secondary antibodies and streptavidin/biotin complex were applied for 30 min each (ZYMED, San Francisco CA), followed by 8 min incubation in diaminobenzidine substrate and extensive washing. Sections were lightly counter-stained in hematoxylin and mounted under a coverslip. Sections were photographed with a Nikon photomicroscope.

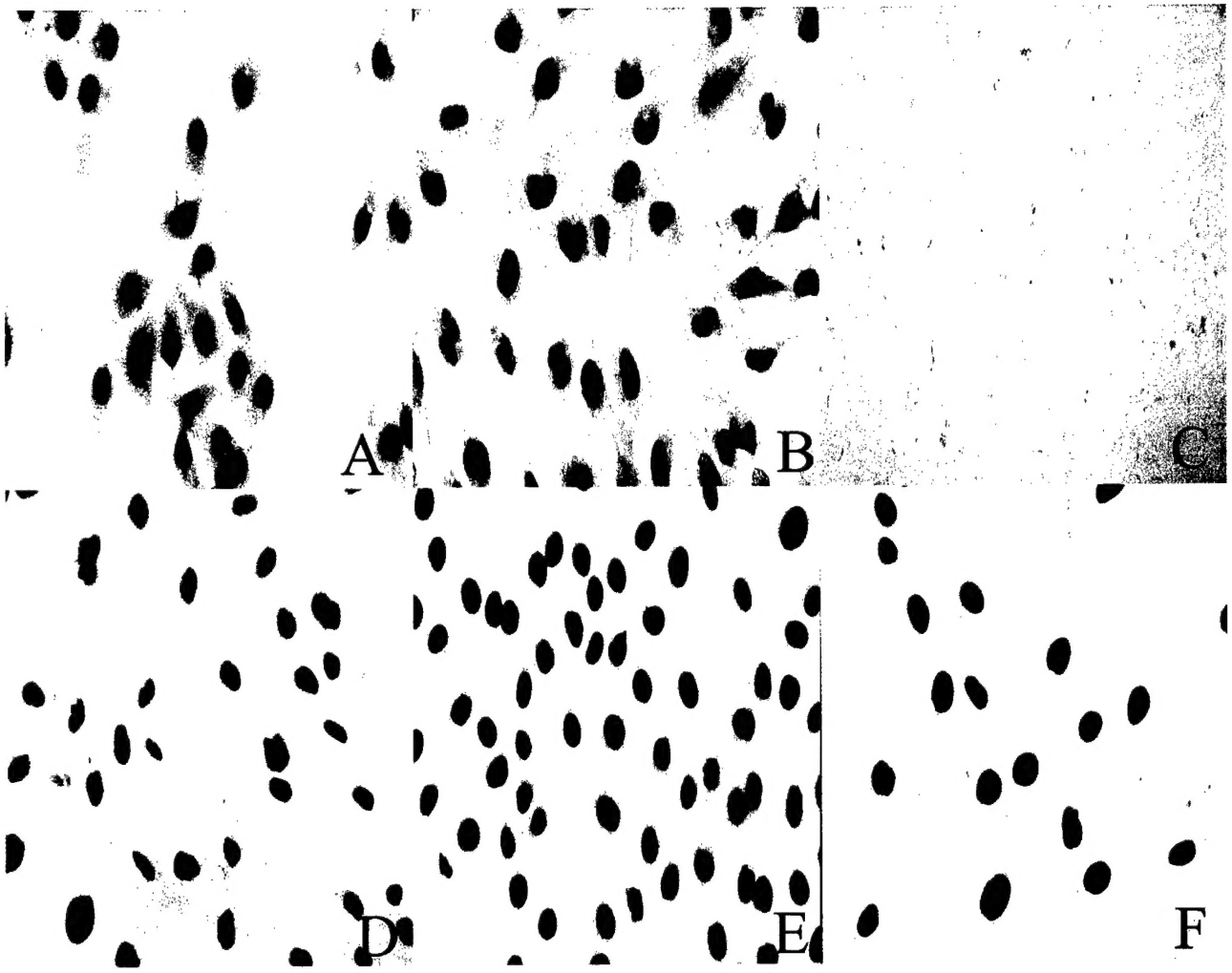


**Figure 2. Expression of NHEJ repair proteins in cultured human cell lines.** DNA-PK in A) HeLa; B) MO59K; C) MO59J and D) Hs 574.T cells. Ku-80 in E) HeLa and F) Hs 574.T cells. M059J cells lack DNA-PKcs protein due to a mutation in the *PRKDC* gene. Methods are as described in Fig 1. Similar results were obtained for XRCC4, Ligase IV and the NBS1/Rad50/MRE11 complex proteins (data not shown).

# Appendix I

DAM17-00-1-0168
Carl W. Anderson

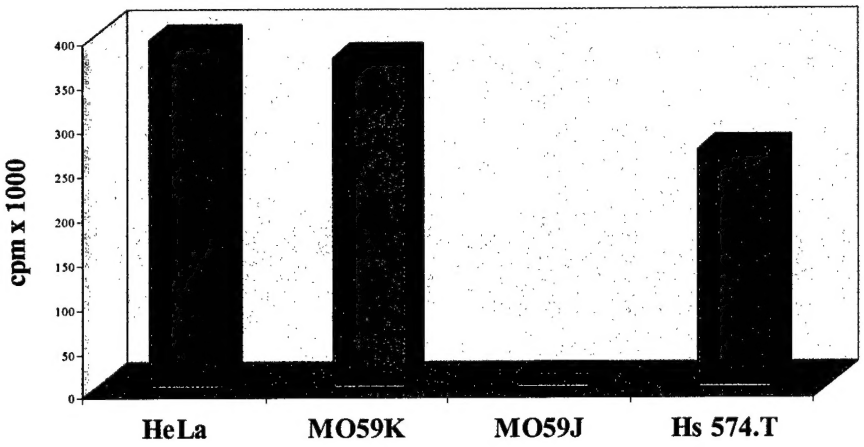


**Figure 3. DNA-PK activity in different human cell lines.** DNA-PK activity assayed in HeLa, MO59K, MO59J and Hs 574.T cells by the'DNA pull-down' assay (Achari et al. 1999). Whole cell extracts were prepared by a modification of the method of Finnie et al.(1995). Briefly $10^7$ cells were harvested, washed 3 times in PBS and the cell pellets were frozen at -80°C. Frozen cell pellets were resuspended in LSB pH 7.2 (10mM HEPES, 25mM KCl, 10mM NaCl, 1mM $MgCl_2$, 0.1mM EDTA) containing 0.1mMDTT and 0.2mM PMSF and centrifuged at 1,000 x g for 10 min. The pellets were resuspended again with 2.5 x the packed cell volume of LSB and incubated on ice for 10 min to allow the cells swell; they were then frozen by plunging them into liquid $N_2$. The cell extracts were then quick thawed at 37°C in the presence of protease inhibitors (0.5mM PMSF, 2 μg/ml each leupeptin and aprotinin), 200μl were removed and adjusted to 0.5M NaCl, 10mM $MgCl_2$ by the addition of 22 μl 5M NaCl, 100mM $MgCl_2$, 5mM DTT (Extraction Buffer, ExB). Extracts were incubated on ice for 3 min and then centrifuged at 10,000 x g for 3min at 4°C. Supernatants were removed and the pellets were extracted with 40 μl of 1/10 dilution of ExB (in 50mM HEPES, pH 7.5) and pooled with the first supernatant. These whole cell extracts were then aliquoted, quick frozen and stored at -80°C until assayed. Protein concentrations were determined by the Bradford assay using BSA as a standard, and cell extracts equivalent to 0.5 mg protein were incubated with 50 μl preswollen dsDNA-cellulose beads (Amersham Pharmacia Biotech, Piscataway, NJ) for 30 min at 4°C. The dsDNA-cellulose was washed three times with 1 ml of buffer A (25 mM HEPES, pH 7.9, 50 mM KCl, 10 mM $MgCl_2$, 5% (v/v) glycerol, 0.5 mM EDTA, 0.25 mM EGTA, and 1 mM DTT) before it was resuspended in 50 μl distilled water; then assays were performed using the SignaTECT DNA-PK assay system (Promega, Madison, WI). Kinase reactions were conducted with 6-12μl aliquots of the resuspended DNA-PK-absorbed cellulose beads and were performed in both the presence and absence of a biotinylated DNA-PK p53-derived substrate peptide. Terminated reactions were analyzed by spotting onto $SAM^2$ membranes, washing, and counting the incorporated radioactivity in a scintillation counter as per the manufacturer's instructions. All assays were performed in duplicate with at least three different extract preparations. The kinase activity was normalized to total protein content. Results shown are from a representative of three experiments.

# DIFFERENTIAL EXPRESSION OF DNA DOUBLE STRAND BREAK REPAIR PROTEINS IN HUMAN BREAST CELLS

**Mangala Tawde, Paul Freimuth and Carl W. Anderson**

Biology Department, Brookhaven National Laboratory, Upton, NY-11953

E-mail:cwa@bnl.gov

DNA double-strand break (DSB) repair is critical for cell survival and for preventing genomic rearrangements that lead to cancer. In mammalian cells, non-homologous end joining (NHEJ), which requires the DNA-dependent protein kinase complex (DNA-PKcs, Ku70, Ku80), XRCC4 and Ligase IV, is the major pathway for DSB repair. In vertebrates, DNA-PKcs, the catalytic component of DNA-PK, is an essential pathway component.

Recent studies of mice found lower levels of DNA-PKcs expression in breast tissue compared to other mouse tissues. Furthermore, BALB/c mice, which are 20 times more susceptible to low dose radiation-induced breast cancer than the most other mouse strains (eg. C57Bl/6), expressed less DNA-PKcs protein than radiation-resistant strains. Thus, breast cancer susceptibility has been associated with DNA DSB repair capacity, radiosensitivity and DNA-PKcs expression. Cell lines from more than 40 % of cancer patients exhibit increased genomic instability. However no correlation has yet been made between radiosensitivity in cancer patients and the expression and activities of DNA repair proteins in fibroblast cell lines derived from these patients.

Our earlier studies showed that DNA-PKcs was differentially expressed in normal and malignant human tissues, with highest levels in neurons and glial cells and lowest in liver and resting breast tissues. All tissues showed similar mRNA content for the protein suggesting the poor expression of DNA-PK could result from post-transcriptional mechanisms rather than transcriptional regulation. When the above observations were recapitulated by studying selected human tissue sections by immunohistochemistry (IHC) for expression of the NHEJ proteins, a striking cell-to-cell specificity was observed. Epithelial cells showed strong staining while stromal cells exhibited very little NHEJ protein expression. To model these *in-vivo* findings *in-vitro*, a cell line of breast stromal origin (Hs 574.T; ATCC CRL-7345) is being characterized for expression of all NHEJ repair proteins by immunohistochemistry, immunofluorescence, and immunoblotting using prepared and commercial antisera specific for each of the NHEJ proteins. Preliminary studies have shown lower activity but comparable expression of DNA-PKcs and the Ku subunits in this cell line. The XRCC4/Lig IV activity, and the genome instability of these cells also is under investigation. Cell lines derived from breast tumors are being examined for polymorphisms in the coding sequences of the NHEJ genes.

Supported by the U.S. Army Medical Research and Material Command under DAMD17-00-1-0168.

*letter*

# Amplification of *PPM1D* in human tumors abrogates p53 tumor-suppressor activity

Dmitry V. Bulavin[1], Oleg N. Demidov[2], Shin'ichi Saito[2], Paivikki Kauraniemi[3,4], Crissy Phillips[1], Sally A. Amundson[1], Concetta Ambrosino[5], Guido Sauter[6], Angel R. Nebreda[5], Carl W. Anderson[7], Anne Kallioniemi[3], Albert J. Fornace Jr[1] & Ettore Appella[2]

Published online: 20 May 2002, DOI: 10.1038/ng894



**Expression of oncogenic Ras in primary human cells activates p53, thereby protecting cells from transformation. We show that in Ras-expressing IMR-90 cells, p53 is phosphorylated at Ser33 and Ser46 by the p38 mitogen-activated protein kinase (MAPK). Activity of p38 MAPK is regulated by the p53-inducible phosphatase PPM1D, creating a potential feedback loop. Expression of oncogenic Ras suppresses PPM1D mRNA induction, leaving p53 phosphorylated at Ser33 and Ser46 and in an active state. Retrovirus-mediated overexpression of PPM1D reduced p53 phosphorylation at these sites, abrogated Ras-induced apoptosis and partially rescued cells from cell-cycle arrest. Inactivation of p38 MAPK (the product of *Mapk14*) *in vivo* by gene targeting or by PPM1D overexpression expedited tumor formation after injection of mouse embryo fibroblasts (MEFs) expressing E1A+Ras into nude mice. The gene encoding PPM1D (*PPM1D*, at 17q22/q23) is amplified in human breast-tumor cell lines and in approximately 11% of primary breast tumors, most of which harbor wildtype p53. These findings suggest that inactivation of the p38 MAPK through PPM1D overexpression resulting from *PPM1D* amplification contributes to the development of human cancers by suppressing p53 activation.**

Activation of the p53 tumor-suppressor protein by different stresses causes cell-cycle arrest and apoptosis[1,2], or may result in a permanent cell-cycle arrest that is indistinguishable from senescence[3,4]. Whereas transient, p53-dependent cell-cycle arrest after genotoxic stress may provide additional time for DNA repair, apoptosis and senescence contribute to the suppression of tumor induction. A distinct premature senescence is induced in primary cells in response to super-mitogenic signals such as the expression of oncogenic *HRAS*. In primary mouse cells, Ras-induced cell-cycle arrest is completely dependent on p53; how-

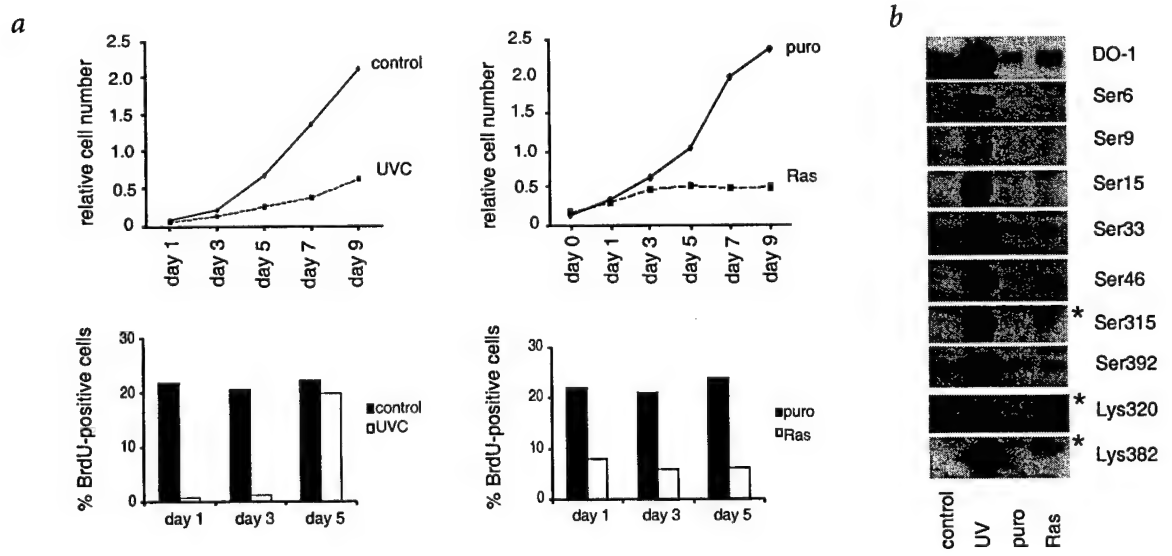


**Fig. 1** Human p53 is phosphorylated at Ser33 and Ser46 after H-rasV12 infection. *a*, Proliferation of IMR-90 cells after no treatment, exposure to UV-C light or infection with pBabe retroviruses expressing either a puromycin-resistance gene alone (puro) or H-rasV12 (Ras) was analyzed with MTS reagent. Average values from three independent experiments are shown. *b*, Western blot showing p53 phosphorylation in IMR-90 cells, using phospho- or acetyl-specific polyclonal antibodies after immunoprecipitation from extracts. Asterisks indicate nonspecific bands.

*[1]Gene Response Section, [2]Laboratory of Cell Biology, National Cancer Institute and [3]Cancer Genetics Branch, National Human Genome Research Institute, National Institutes of Health, Bethesda, Maryland 20892, USA. [4]Laboratory of Cancer Genetics, Institute of Medical Technology, University of Tampere and Tampere University Hospital, Tampere, Finland. [5]European Molecular Biology Laboratory, Meyerhofstrasse 1, Heidelberg, Germany. [6]Institute of Pathology, University of Basel, Basel, Switzerland. [7]Biology Department, Brookhaven National Laboratory, Upton, New York, USA. Correspondence should be addressed to E.A. (e-mail: appellae@pop.nci.nih.gov).*

ever, for human cells, additional mechanisms are involved[3,4]. Nevertheless, oncogenic Ras activates p53-dependent transcription in human cells, indicating the existence of pathways that modulate p53 activity during hyperproliferative stimulation[5]. Increased p53 protein levels after hyperproliferative stimulation requires the p14ARF protein[6,7], which sequesters MDM2, thus permitting p53 accumulation. However, oncogenic Ras did not induce p14ARF accumulation in human diploid fibroblasts such as IMR-90 (ref. 7). Analysis of the p53 post-translational modifications that are required for its full activation[1] should therefore contribute to understanding the effects of oncogenic Ras in normal human cells.

Treatment of IMR-90 primary human lung fibroblasts with UV light (10 J/m$^2$) resulted in substantial apoptosis (up to 50% of cells) during the first 24 hours (data not shown), and subsequent arrest of cell-cycle progression that lasted for at least 3 days (Fig. 1*a*). By the fifth day after exposure, however, these cells reinitiated cell-cycle progression, as determined by analysis of cell growth rates and the number of cells in S phase. Cells infected with an oncogenic H-rasV12–expressing retrovirus vector rapidly arrested cell-cycle progression (Fig. 1*a*), but, in contrast to UV-irradiated cells, these cells never reinitiated growth and thus became prematurely senescent, as confirmed by positive staining for senescence associated β-galactosidase (data not shown).

The p53 protein is a crucial component of both DNA-damage and oncogene-induced responses; the different outcomes may result from differences in post-translational modifications induced by each stimulus. However, the post-translational modifications to p53 after overexpression of H-rasV12 have not been fully characterized. Using a panel of antibodies specific for phosphorylated or acetylated p53, we found that UV-irradiated IMR-90 cells accumulated p53 that was modified at most known sites, except Thr18, Ser20 and Ser37 (see Fig.1*b* and Web Fig. A online). By contrast, although retrovirus-mediated expression of H-rasV12 induced p53 accumulation, in this case p53 was phosphorylated at two sites, Ser33 and Ser46. These sites previously were shown to be phosphorylated by p38 MAPK after exposure to UV light[8,9]. Mutations that resulted in changes of both serines to alanine, inactivation of the p38 MAPK with a chemical inhibitor or overexpression of the p38 MAPK-specific phosphatase, PPM1D, have been shown to significantly reduce p53-dependent transcription and apoptosis[8,9]. The pattern of p53 modifications in IMR-90 cells after infection with an H-rasV12–expressing retrovirus was substantially different from that reported for replicative senescence, in which increased phosphorylation was also observed at Ser15 and Thr18 (ref. 10). In contrast to a previous report[3], we did not observe significant phosphorylation at Ser15 of p53. The increased phosphorylation at amino-terminal sites observed in replicative senescence could

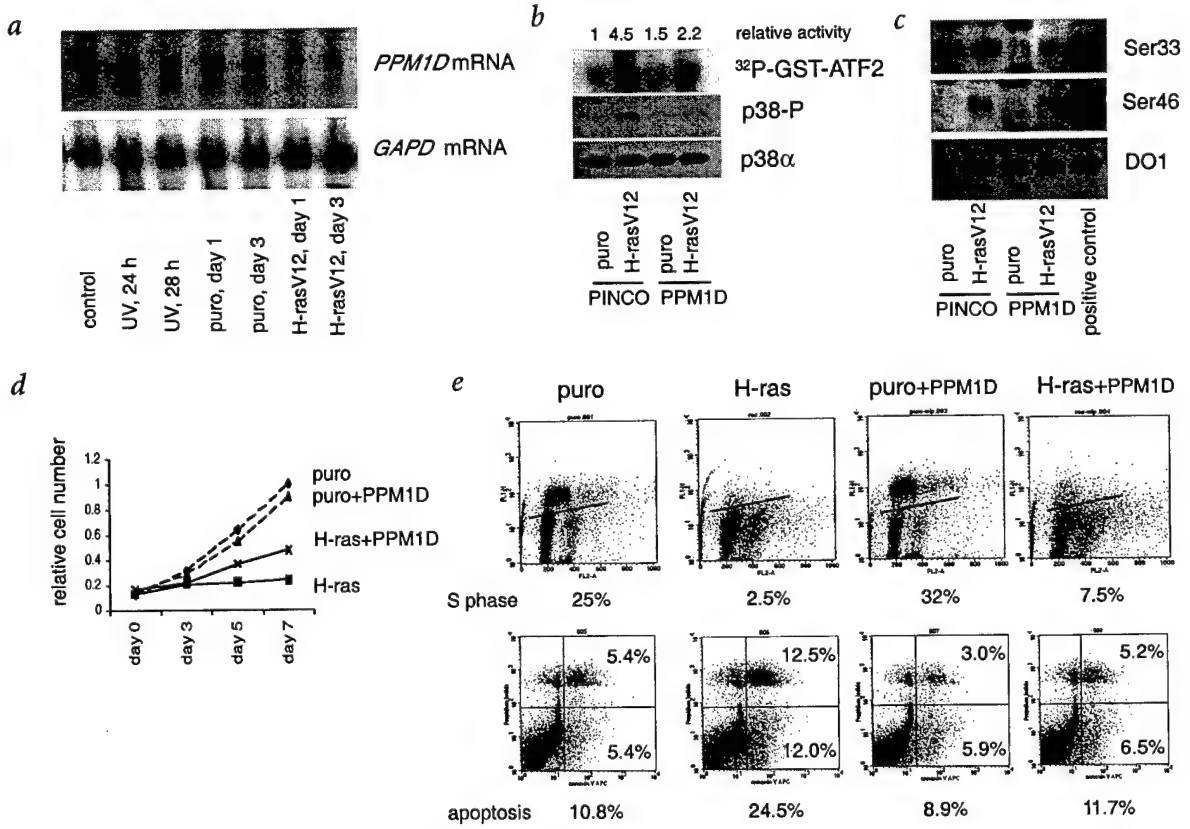


Fig. 2 Overexpression of PPM1D abrogates apoptosis and partially reverses H-rasV12–induced cell-cycle arrest in IMR-90 cells. *a*, Northern blot showing *PPM1D* mRNA levels in IMR-90 cells after exposure to UV light, control retroviral infection (puro) or retrovirus-mediated H-rasV12 expression. *GAPD* expression served as a control. *b*, Analysis of p38 MAPK phosphorylation and activity. *c*, Retrovirus-mediated expression of the PPM1D phosphatase induced by H-rasV12 resulted in decreased p53 phosphorylation at Ser33 and Ser46, as shown using phospho-specific antibodies after p53 immunoprecipitation from total cell protein extracts. The p53 protein from A549 cells exposed to UV light served as a positive antibody control. *d*, PPM1D overexpression partially reversed H-rasV12–induced senescence. Cell number was measured as in Fig. 1a after retrovirus infection of wildtype MEFs with vector (puro), virus expressing H-rasV12, vector and virus expressing PPM1D (puro+PPM1D) or virus expressing H-rasV12 and PPM1D. *e*, The number of cells in S phase was analyzed after pulse-labeling with BrdU on day 3 after selection with puromycin. Apoptosis was analyzed after harvesting cells (see Methods). Percent apoptosis was determined from the cells in the bottom right (PI-negative, annexin V–positive cells, 'early' apoptosis) and top right (PI-positive, annexin V–positive cells, 'late' apoptosis) areas.

result from the creation of uncapped telomeres, which may induce a DNA damage–like modification pattern through activation of kinases involved in response to genotoxic stress. Our finding that primarily Ser33 and Ser46 of p53 were phosphorylated after infection by an H-rasV12–expressing retrovirus suggests that many of the kinases activated in response to genotoxic stress are not activated in this case.

To inactivate p53 and re-initiate cell-cycle progression after stress, cells must have mechanisms that inactivate stress-activated kinases. It has been suggested[9] that activation of the p38 stress kinase is inhibited by the action of PPM1D phosphatase. PPM1D expression is induced in response to genotoxic stress in a p53-dependent manner[11]; thus, exposure of IMR-90 cells to UV-light induced *PPM1D* mRNA accumulation, with maximum expression at 24 to 28 hours (Fig. 2*a*). This maximum correlated with the decrease of phosphorylation of p53 at Ser33 and Ser46 to basal levels by 48 hours after UV treatment. In contrast to the dynamic changes in the phosphorylation of Ser33 and Ser46 in response to UV light, after H-rasV12 infection phosphorylation at these sites was constant (Fig. 1*b*), consistent with continuous, steady-state phosphorylation by activated p38 MAPK. However, no change was observed in the level of *PPM1D* mRNA (Fig. 2*a*) after infection by the H-rasV12–expressing retrovirus, despite the fact that p53 is activated under these conditions. Thus, another mechanism must prevent activation of PPM1D transcription after Ras overexpression, although it is not regulated by the Raf/MEK1/Erk pathway, as treatment of IMR-90 cells with the MEK1 inhibitor, PD98059, did not induce *PPM1D* mRNA accumulation (data not shown). Nevertheless, we considered whether PPM1D overexpression could overcome oncogenic Ras-induced responses.

**Table 1 • Effect of PPM1D on oncogene transformation[a]**

| Genotype | Retrovirus | Growth in soft agar[b] |
|---|---|---|
| wildtype | puro | – |
| | H-rasV12 | – |
| | Neu | – |
| | Myc | – |
| | PPM1D | – |
| | H-rasV12 + PPM1D | + |
| | Neu + PPM1D | + |
| | Myc + PPM1D | + |
| | Ras + Myc | ++ |
| | Ras + Neu | + |
| *Trp53*$^{-/-}$ | puro | – |
| | H-rasV12 | ++ |
| | PPM1D | – |
| | H-rasV12 + PPM1D | ++ |
| | Neu | +++ |
| | Myc | +++ |

[a]Colony formation in 0.5% soft agar was determined 3 wk after infection of wildtype or *Trp53*$^{-/-}$ MEFs with the indicated retroviral vectors. [b]Colonies were scored as: +, 10–30 colonies; ++, 30–100; +++, greater than 100 per well of a six-well plate (see Methods).

First, we examined the effect of PPM1D expression on p38 MAPK activity and the phosphorylation of human p53 at Ser33 and Ser46, sites modified by the p38 MAPK kinase. We

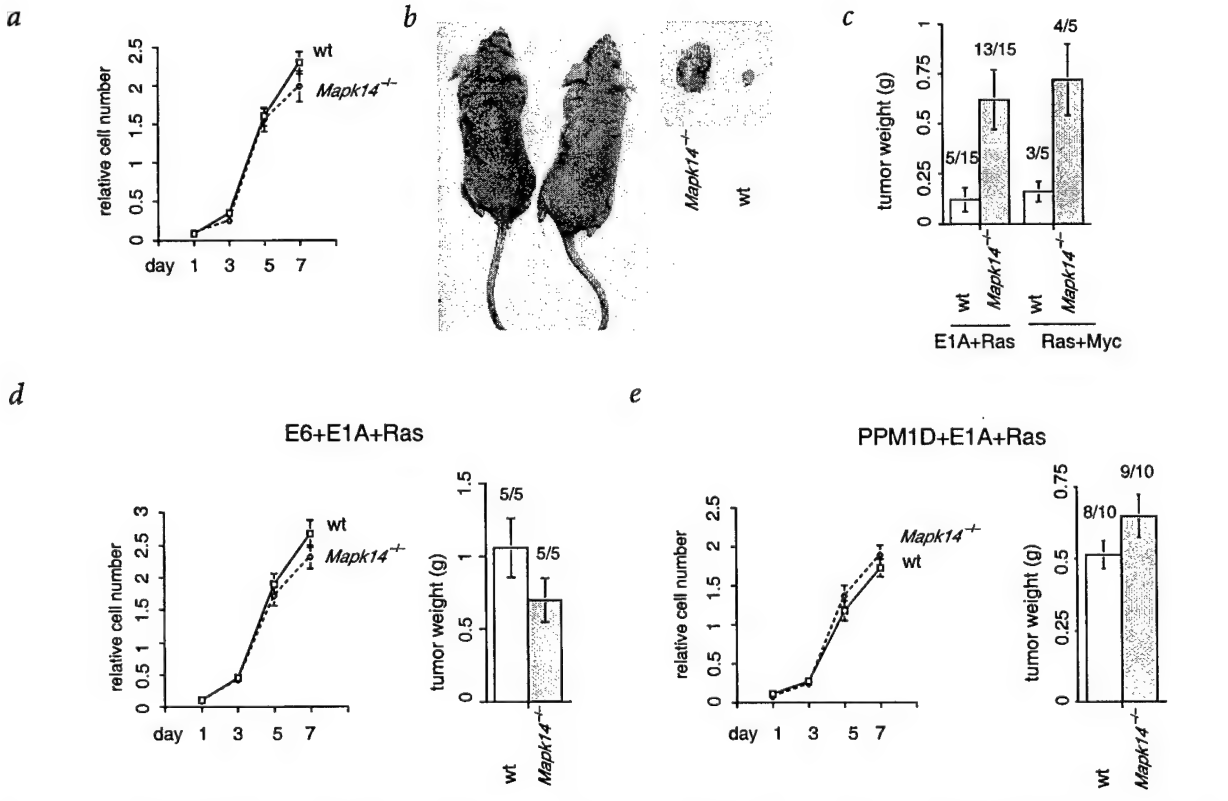


**Fig. 3** PPM1D phosphatase functions in the p38 MAPK/p53 pathway to regulate transformation *in vivo*. *a*, Early-passage (passage 2 or 3) wildtype or *Mapk14*$^{-/-}$ MEFs were infected with E1A and H-Ras–expressing retroviruses, and cell proliferation was analyzed using the MTS test. *b*, BALB/CanNCr-nu male mice at 6–8 wk were injected subcutaneously with wildtype (right side) or *Mapk14*$^{-/-}$ (left side) MEFs expressing E1A and H-ras. Four weeks later, mice were killed and the tumors were weighed. *c*, Results of the same experiment as in *b*, carried out with cells expressing *MYC* and H-*ras*V12 oncogenes. *d*, Same as *a*, but MEFs were infected with HPV-16 E6 to inactivate p53 and then with E1A and H-ras. Tumor size (right panel) was analyzed 16–20 d after injection. *e*, Same as *a*, but MEFs were infected with PPM1D expressing virus to inactivate p38 MAPK and then with E1A and H-rasV12 virus. Tumor size (right panel) was analyzed four weeks later.

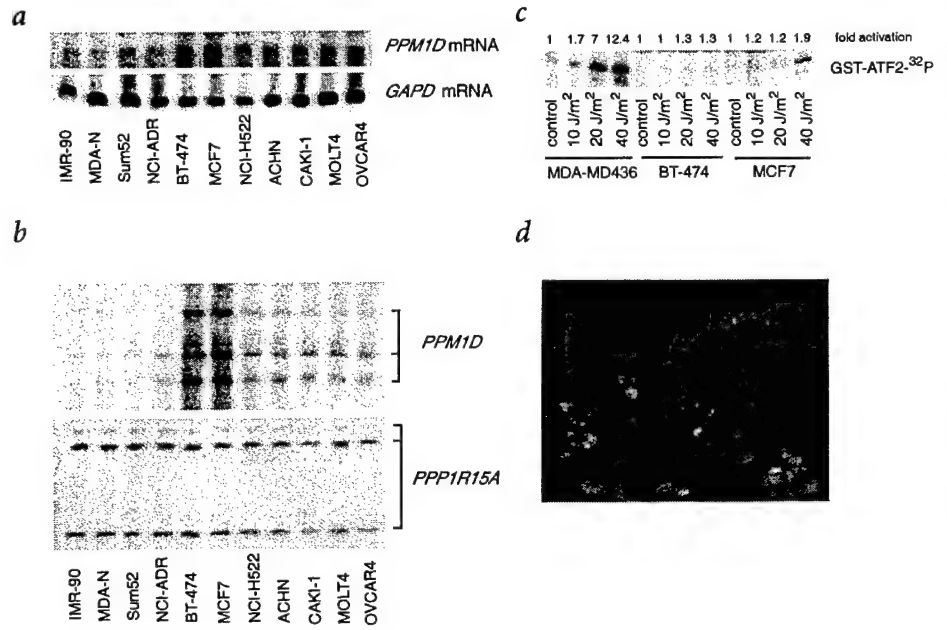


**Fig. 4** *PPM1D* amplification, messenger RNA accumulation and p38 MAPK activation. ***a***, Northern blot showing level of *PPM1D* mRNA, compared with level of *GAPD* mRNA, in human tumor cell lines. ***b***, Southern blot showing amplification of *PPM1D* after digestion of genomic DNA with *Pvu*II. The same blot then was probed with the *PPP1R15A* cDNA to provide a single-copy gene internal control. ***c***, Activation of p38 MAPK in breast cell lines with (BT474 and MCF7) or without (MDA-MB436) *PPM1D* amplification 30 min after irradiation of cells with different doses of UV-C light, determined as in Fig. 2*b*. ***d***, BAC clone RP11-634F5, representing *PPM1D*, was labeled with SpectrumOrange-dUTP and hybridized to a tissue microarray containing primary breast tumor specimens[18]. An example of a tumor specimen with *PPM1D* amplification (red signals) is shown. The nuclei were stained with 4′,6-diamidino-2-phenylindole (blue).

observed inactivation of p38 MAPK in Ras-containing cells after overexpression of PPM1D phosphatase (Fig. 2*b*). The levels of *PPM1D* mRNA were 5.3 to 7.1 times higher in PPM1D-infected IMR-90 cells (data not shown). The p53 protein immunoprecipitated from IMR-90 cells that were co-infected with retroviruses expressing H-rasV12 and PPM1D showed little, if any, phosphorylation at Ser33 or Ser46, compared with cells infected with the H-rasV12–expressing virus alone (Fig. 2*c*). In agreement with previously published data[11], we found that PPM1D phosphatase did not directly dephosphorylate p53 at Ser33 and Ser46 *in vitro*, indicating that the *in vivo* effect of PPM1D on p53 phosphorylation is indirect and results from inactivation of p38 MAPK. Unexpectedly, the p38 MAPK chemical inhibitor, SB202190, which inhibits two of the p38 MAPK isoforms (α and β), failed to reduce p53 phosphorylation at Ser33 and Ser46 in IMR-90 cells expressing H-rasV12 (data not shown). Similar results were described previously for the UV-induced phosphorylation of p53 at Ser46 (ref. 9), indicating a role for SB202190-insensitive isoforms of p38 in regulating p53 phosphorylation. H-rasV12 and PPM1D co-infected cells also showed an intermediate growth rate, compared with IMR-90 cells infected either with a control retrovirus expressing only a puromycin-resistance gene (*puro*$^r$) or with the PPM1D-expressing virus alone (Fig. 2*d*). Further analysis of BrdU-positive cells revealed that PPM1D overexpression only partially prevented Ras-induced cell-cycle arrest (Fig. 2*e*); however, oncogene-induced apoptosis was almost completely abrogated in IMR-90 cells expressing PPM1D and Ras (Fig. 2*e*). Thus, expression of PPM1D in IMR-90 cells abrogated p53 phosphorylation at Ser33 and Ser46, protected cells from Ras-induced apoptosis and also partially prevented cell-cycle arrest induced by H-rasV12, which is consistent with the fact that this arrest is only partially dependent on p53 in human cells[3,4].

Proteins that inactivate p53 are potential proto-oncogenes. To determine whether *PPM1D* has oncogenic potential, we co-infected retroviruses containing *PPM1D* and different oncogenes, including *H-rasV12*, *MYC* or *NEU1*, into wildtype MEFs and then analyzed anchorage-independent growth and ability to form foci in soft agar (see Table 1 and Web Fig. B online). In both assays, *PPM1D* complemented H-rasV12 for transformation of wildtype MEFs, confirming that *PPM1D* is a proto-oncogene. Overexpression of PPM1D also complemented *MYC* and *NEU1* (Table 1), indicating the potential importance of PPM1D for a wider range of tumors.

One mechanism through which PPM1D may function in combination with Ras is by preventing activation of p38 MAPK (Fig. 2*b*)[9]. The p38 MAPK protein is involved in several growth inhibitory activities, as it regulates cyclin D levels, p53 activation and the activity of Cdc25B phosphatase[8,12]. Inactivation of the kinase by PPM1D would thus prevent p38 MAPK–mediated growth inhibition. To characterize the pathway that is crucial for PPM1D-induced transformation *in vitro*, we considered whether *PPM1D* could transform *Trp53*$^{-/-}$ MEFs, as was the case for H-rasV12 expression. However, neither colony formation nor growth in soft agar (see Table 1 and Web Fig. B online) was observed after infection of *Trp53*$^{-/-}$ MEFs with *PPM1D*-expressing virus, indicating that PPM1D overexpression did not cause cell transformation. This result suggests that p53 and PPM1D function in the same pathway for cell transformation and supports the idea that p53 is a primary target for PPM1D in the induction of *in vitro* transformation caused by H-rasV12.

As escape from cell-cycle arrest, apoptosis and senescence controls are required for oncogene-induced cellular transformation *in vivo*, we examined the effect of PPM1D expression on the tumorigenic potential of *Mapk14*$^{-/-}$ MEFs. Wildtype and *Mapk14*$^{-/-}$ MEFs were infected with retroviruses encoding the adenovirus E1A-12S gene and activated H-rasV12. Co-expression of both oncogenes results in few, if any, tumors after injection of wildtype MEFs into nude mice. However, if p53 activity is suppressed, tumor formation is facilitated[13]. Expression of E1A and *Hras* mRNA, as quantified by dot-blot hybridization, was similar for both wildtype and *Mapk14*$^{-/-}$ retrovirus-infected MEF cells (data not shown), as were their growth rates in culture (Fig. 3*a*). We found relatively few tumors when wildtype cells expressing both oncogenes were injected into nude mice (5 tumors/15 mice), but most animals injected with *Mapk14*$^{-/-}$ MEFs expressing both oncogenes developed tumors (13 tumors/15 mice; Fig. 3*b*,*c*). Moreover, the tumors produced

by E1A+Ras–transformed *Mapk14*$^{-/-}$ MEFs were substantially larger than those from mice injected with E1A+Ras–transformed wildtype MEFs (Fig. 3*b*,*c*). Similar data were obtained with cells expressing the *MYC* and H-*ras*V12 oncogenes (Fig. 3*c*). These findings demonstrate that p38α is required to suppress tumor formation *in vivo*.

If p38 MAPK functions through the p53 tumor-supressor pathway, removing p53 through expression of HPV-16 E6 should eliminate the difference in the abilities of oncogene-expressing wildtype and *Mapk14*$^{-/-}$ MEFs to form tumors. Indeed, when both cell types were infected with HPV-16 E6 and then with E1A+Ras oncogenes, no significant difference in tumor appearance and size was found between wildtype and *Mapk14*$^{-/-}$ cells (see Fig. 3*d* and Web Fig. C online). We then introduced PPM1D phosphatase into E1A+Ras MEFs and monitored tumor formation after injection of nude mice. Similar to HPV-16 E6, overexpression of PPM1D phosphatase significantly reduced the difference in tumor formation between wildtype and *Mapk14*$^{-/-}$ MEFs (see Fig. 3*e* and Web Fig. C online). These data suggest that PPM1D, p38 MAPK and p53 function in the same pathway to regulate tumor formation *in vivo*.

To determine whether PPM1D is required for tumor suppression in human tissues, we analyzed *PPM1D* mRNA expression levels in 64 human tumor cell lines (see Web Table A online)[14]. Compared with IMR-90 cells, levels of *PPM1D* mRNA were 4.7 to 9.4 times higher in the 4 breast-tumor cell lines MDA-MB361, BT474, MCF-7 and KPL-1; data for BT474 and MCF-7 and 8 lines with normal *PPM1D* mRNA levels are shown in Fig. 4*a*. In all cases, the size of the *PPM1D* mRNA, as determined by northern-blot analysis, was the same as that predicted (2.9 kb), confirming that the gene product is not grossly altered in tumors. In addition, the sequence of the PPM1D cDNA from MCF7 and several other tumor cell lines, obtained after RT–PCR of total RNA, was unaltered (data not shown).

We localized *PPM1D* to chromosome 17q22/q23 by FISH analysis (data not shown), which is consistent with the location of the gene within the draft sequence of the human genome. The chromosomal region 17q22/q24 is frequently amplified in primary breast tumors[15]. Moreover, this amplification has been associated with a poor prognosis for individuals with breast cancer, suggesting that genes affected by this amplification may be important in breast cancer progression. Southern-blot analysis of genomic DNA after digestion with *Pvu*II showed that *PPM1D* was amplified in the breast-cancer cell lines with elevated *PPM1D* mRNA levels, but not in several other cell lines with normal levels of *PPM1D* mRNA (Fig. 4*b*). The amplification pattern of the digestion fragments indicates that the structure of *PPM1D* was not altered in the tumor cell lines tested; thus, the amplicons should contain several full copies of the gene encoding PPM1D.

Consistent with the role of PPM1D phosphatase in negative regulation of p38 MAPK (Fig. 2*b*)[9], UV-induced early activation of p38 MAPK was significantly attenuated during the first 30 minutes in breast cell lines in which the PPM1D gene was amplified and overexpressed (BT-474 and MCF7), compared with a breast cell line (MDA-MB435) without PPM1D amplification (Fig. 4*c*). Nonetheless, p53 in MCF7 cells was still phosphorylated at Ser33 and Ser46 after UV radiation, implying that several kinases could regulate phosphorylation of these sites after DNA damage[16,17].

To assess the significance of PPM1D expression in human cancer, we extended our analysis to human primary breast tumors by determining *PPM1D* amplification with tissue microarray technology[18]. This analysis showed that the *PPM1D* region was amplified in 37 of the 326 (11.3%) tumors tested (Fig. 4*d*). To confirm the connection between *PPM1D* amplification and mRNA levels, we quantified the relative level of *PPM1D* mRNA in total RNA from 11 tumor samples using real-time PCR. Overexpression of *PPM1D* mRNA was confirmed for seven of the eight samples containing *PPM1D* amplification. None of three tested tumors without *PPM1D* amplification showed an increase in *PPM1D* mRNA levels. Subsequent analysis of the p53 sequence after RT–PCR showed that only one tumor with amplified *PPM1D* had a mutation (cgc→cac at codon 174; Arg→His), suggesting that *PPM1D* amplification occurs commonly in tumors containing wildtype p53.

Whereas *TP53* is inactivated by mutation in approximately half of all human tumors, p53 function is widely believed to be abrogated in most, if not all, tumors, including those with wildtype *TP53* (ref. 19). However, the mechanisms that prevent p53 activation in these cases are incompletely characterized. Previous studies showed that silencing of *CDKN2A* by methylation[20], deletion of a portion of *CDKN2A* (ref. 21) or amplification of *MDM2* (ref. 22) are common mechanisms responsible for inactivating wildtype p53 in human tumors. In addition, p53 may be kept in an inactivated state in some tumors, including those from breast, colon and neural tissues, by cytoplasmic sequestration or silencing of its expression[23,24]. Several types of tumors do not fall into the above categories, however, suggesting the existence of additional mechanisms. The data presented here indicate that PPM1D overexpression prevents phosphorylation of p53 at Ser33 and Ser46, inhibiting its activation in H-rasV12–transfected cells. PPM1D overexpression thus rescues cells from apoptosis and partially from cell-cycle arrest induced by H-rasV12, promoting cell transformation *in vitro* and *in vivo*. In agreement with a role for PPM1D phosphatase as a positive regulator of proliferation, cells established from *Ppm1d*$^{-/-}$ mice show decreased proliferation rates[25] and have p38 MAPK constitutively phosphorylated at activating sites (see Web Fig. D online).

The gene *PPM1D* is amplified and overexpressed in some human breast tumors with wildtype p53. Although we do not completely exclude other possible targets, our results support the hypothesis that PPM1D phosphatase is a candidate proto-oncogene that may be involved in tumorigenesis through inactivation of p53. Though *HRAS* mutations are quite rare in breast cancer, we show that *PPM1D* also complements other growth-promoting oncogenes, including *NEU1*, which is amplified and overexpressed in about 50% of breast tumors[26], further supporting the significance of our findings with respect to the mechanisms by which p53 is inactivated in human tumors. Our findings as well as those of Li *et al.*[27] indicate that, similar to *MDM2* amplification, amplification of *PPM1D* contributes to the development of human cancer. PPM1D thus represents a promising new target for cancer therapy.

## Methods

**Cell cultures and retrovirus infection.** IMR-90 primary cells (ATCC CCL-186), mouse embryo fibroblasts (MEFs) and Phoenix Eco/Ampho packaging cell lines were grown in Dulbecco's modified Eagle's medium (DME) with 10% fetal calf serum at 37 °C in a humidified atmosphere of 5% $CO_2$ in air. Cell lines from the National Cancer Institute screening panel[14] were grown either in DME or RPMI medium. For retrovirus production, we transfected packaging cells with the designated plasmids using Lipofectamin2000 reagent (GIBCO/Invitrogen) and infected target cells as described previously[8]. We used cells for experimentation (day 0) after selection for 4 d in the presence of 2 μg ml$^{-1}$ puromycin. Cell growth was analyzed using the MTS reagent (3-(4,5-dimethylthiazol-2-yl)-5-(3-carboxymethoxyphenyl)-2-(4-sulfophenyl)-2H-tetrazolim, inner salt, Promega). We determined the number of cells in S phase after BrdU labeling as described[28].

**Plasmids.** We cloned PPM1D cDNA into the PINCO vector using *Bam*HI/*Not*I sites. pBabe-puro and pBabe-H-rasV12 vectors were provided by S. Lowe (Cold Spring Harbor Laboratory). The IRES c-myc (human)

retrovirus vector pBabeMNIRESgfpmyc[29] was provided by L.Z. Penn (Toronto Univ.), and pBabe-c-neu (rat)[30] was obtained from P. Sicinski (Dana-Farber Cancer Institute).

**Analysis of p53 and p38 phosphorylation.** We analyzed p53 phosphorylation after p53 immunoprecipitation of 1 mg of protein extract as described[31]. Affinity-purified, phosphorylation site–specific antibodies have been described or were purchased from a commercial supplier (New England Biolabs).

We analyzed p38 MAPK phosphorylation using a phospho-specific antibody that specifically recognizes the phosphorylated, active form of p38 MAPK. We determined kinase activity with a kit that is specific primarily for the p38α isoform (Cell Signaling Technology).

**Colony formation assay and cloning in soft agar.** Suppression of colony formation was determined 2–3 wk after infection of MEFs in 100-mm dishes with the designated retroviruses. Colonies were selected with 500 μg $ml^{-1}$ G418, then fixed and stained with 0.1% crystal violet. For soft agar cloning, we seeded 20,000 puromycin-selected, infected cells in 0.5% agar into each well of 6-well plates. Samples were analyzed in triplicate.

**Real-time PCR and mRNA analysis.** We extracted total RNA from 11 primary breast tumors using the RNeasy kit (Qiagen). We determined *PPM1D* mRNA levels relative to those for *GAPD* and *PPP1R15A* in primary breast tumors after reverse transcription coupled to the real-time PCR (primers available upon request) using an ABI PRISM 7700 Sequence Detection System and the SYBR Green PCR Master Mix. We analyzed mRNA levels in the panel of human tumor cell lines using a dot-blot procedure; polyU served as a control for relative mRNA content.

**Analysis of p53 for mutations.** To verify the p53 sequence in primary breast tumors, we amplified cDNAs obtained after reverse transcription and sequenced both strands of the PCR products.

**Tissue microarray analysis of *PPM1D*.** We used the BLASTN program to localize *PPM1D* to three overlapping BAC clones (RP11-15E18, RP11-634F5 and RP11-1081E4) in the draft human genome sequence that map to 17q23. BAC clone RP11-634F5, representing *PPM1D*, labeled with SpectrumOrange-dUTP, and a centromere-specific, SpectrumGreen-dUTP-labeled chromosome 17 probe were hybridized to a tissue microarray containing primary breast tumors[18]. Nuclei were stained with 4′, 6-diamidino-2-phenylindole. Tumor samples with at least a threefold increase in the number of *PPM1D* signals, as compared with chromosome 17 centromere signals, were considered to be amplified.

All tumor specimens evaluated were anonymous, archival tissue specimens. The use of these specimens for retrospective analyses was approved by the Ethics Committee of the University of Basel, and their use for tissue microarray analysis was approved by the Institutional Review Board of the National Institutes of Health.

*Note: Supplementary information is available on the Nature Genetics website.*

**Acknowledgments**

*We are grateful to J. Hildesheim for help with real-time PCR, J. Clark for help with DNA sequencing and T. Dennis for help with FISH analysis. This study was supported in part by a US Army Breast Cancer Idea Award (to C.W.A.) at the Brookhaven National Laboratory under contract with the US Department of Energy.*

**Competing interests statement**

*The authors declare that they have no competing financial interests.*

Received 16 January; accepted 22 April 2002.

1. Appella, E. & Anderson, C.W. Post-translational modifications and activation of p53 by genotoxic stresses. *Eur. J. Biochem.* **268**, 2764–2772 (2001).
2. Vogelstein, B., Lane, D. & Levine, A.J. Surfing the p53 network. *Nature* **408**, 307–310 (2000).
3. Lin, A.W. *et al.* Premature senescence involving p53 and p16 is activated in response to constitutive MEK/MAPK mitogenic signaling. *Genes Dev.* **12**, 3008–3019 (1998).
4. Zhu, J., Woods, D., McMahon, M. & Bishop, J.M. Senescence of human fibroblasts induced by oncogenic Raf. *Genes Dev.* **12**, 2997–3007 (1998).
5. Ferbeyre, G. *et al.* PML is induced by oncogenic *ras* and promotes premature senescence. *Genes Dev.* **14**, 2015–2027 (2000).
6. Palmero, I., Pantoja, C. & Serrano, M. $p19^{ARF}$ links the tumour suppressor p53 to Ras. *Nature* **395**, 125–126 (1998).
7. Wei, W., Hemmer, R.M. & Sedivy, J.M. Role of $p14^{ARF}$ in replicative and induced senescence of human fibroblasts. *Mol. Cell. Biol.* **21**, 6748–6757 (2001).
8. Bulavin, D.V. *et al.* Phosphorylation of human p53 by p38 kinase coordinates N-terminal phosphorylation and apoptosis in response to UV radiation. *EMBO J.* **18**, 6845–6854 (1999).
9. Takekawa, M. *et al.* p53-inducible Wip1 phosphatase mediates a negative feedback regulation of p38 MAPK-p53 signaling in response to UV radiation. *EMBO J.* **19**, 6517–6526 (2000).
10. Webley, K. *et al.* Posttranslational modifications of p53 in replicative senescence overlapping but distinct from those induced by DNA damage. *Mol. Cell. Biol.* **20**, 2803–2808 (2000).
11. Fiscella, M. *et al.* Wip1, a novel human protein phosphatase that is induced in response to ionizing radiation in a p53-dependent manner. *Proc. Natl Acad. Sci. USA* **94**, 6048–6053 (1997).
12. Bulavin, D.V. *et al.* Initiation of a G2/M checkpoint after ultraviolet radiation requires p38 kinase. *Nature* **411**, 102–107 (2001).
13. Jimenez, G.S. *et al.* A transactivation-deficient mouse model provides insights into Trp53 regulation and function. *Nature Genet.* **26**, 37–43 (2000).
14. O'Connor, P.M. *et al.* Characterization of the p53 tumor suppressor pathway in cell lines of the National Cancer Institute anticancer drug screen and correlations with the growth-inhibitory potency of 123 anticancer agents. *Cancer Res.* **57**, 4285–4300 (1997).
15. Tirkkonen, M. *et al.* Molecular cytogenetics of primary breast cancer by CGH. *Genes Chromosom. Cancer* **21**, 177–184 (1998).
16. Hofmann, T.G. *et al.* Regulation of p53 activity by its interaction with homeodomain-interacting protein kinase-2. *Nature Cell Biol.* **4**, 1–10 (2002).
17. D'Orazi, G. *et al.* Homeodomain-interacting protein kinase-2 phosphorylates p53 at Ser 46 and mediates apoptosis. *Nature Cell Biol.* **4**, 11–19 (2002).
18. Kononen, J. *et al.* Tissue microarrays for high-throughput molecular profiling of tumor specimens. *Nature Med.* **4**, 844–847 (1998).
19. Woods, D.B. & Vousden, K.H. Regulation of p53 function. *Exp. Cell Res.* **264**, 56–66 (2001).
20. Esteller, M. *et al.* Hypermethylation-associated inactivation of $p14^{ARF}$ is independent of $p16^{INK4a}$ methylation and *p53* mutational status. *Cancer Res.* **60**, 129–133 (2000).
21. Ho, G.H. *et al.* Genetic alterations of the $p14^{ARF}$-hdm2-p53 regulatory pathway in breast carcinoma. *Breast Cancer Res. Treat.* **65**, 225–232 (2001).
22. Oliner, J.D., Kinzler, K.W., Meltzer, P.S., George, D.L. & Vogelstein, B. Amplification of a gene encoding a p53-associated protein in human sarcomas. *Nature* **358**, 80–83 (1992).
23. Moll, U.M., LaQuaglia, M., Benard, J. & Riou, G. Wild-type p53 protein undergoes cytoplasmic sequestration in undifferentiated neuroblastomas but not in differentiated tumors. *Proc. Natl Acad. Sci. USA* **92**, 4407–4411 (1995).
24. Raman, V. *et al.* Compromised HOXA5 function can limit p53 expression in human breast. *Nature* **405**, 974–978 (2000).
25. Choi, J. *et al.* Mice deficient for the wild-type p53-induced phosphatase gene (*Wip1*) exhibit defects in reproductive organs, immune function, and cell cycle control. *Mol. Cell Biol.* **22**, 1094–1105 (2002).
26. Bièche, I. & Lidereau, R. Genetic alterations in breast cancer. *Genes Chromosom. Cancer* **14**, 227–251 (1995).
27. Li, J. *et al.* Oncogenic properties of *PPM1D* located within a breast cancer amplification epicenter at 17q23. *Nature Genet.* **31** (2002); advanced online publication, 20 May 2002 (DOI: 10.1038/ng888).
28. Bulavin, D.V., Tararova, N.D., Aksenov, N.D., Pospelov, V.A. & Pospelova, T.V. Deregulation of $p53/p21^{Cip1/Waf1}$ pathway contributes to polyploidy and apoptosis of E1A+cHa-ras transformed cells after γ-irradiation. *Oncogene* **18**, 5611–5619 (1999).
29. Oster, S.K. *et al.* Myc is an essential negative regulator of platelet-derived growth factor. *Mol. Cell. Biol.* **20**, 6768–6778 (2000).
30. Bargmann, C.I., Hung, M.C. & Weinberg, R.A. Multiple independent activations of the *neu* oncogene by a point mutation altering the transmembrane domain of p185. *Cell* **45**, 649–657 (1986).
31. Saito, S. *et al.* ATM mediates phosphorylation at multiple p53 sites, including Ser46, in response to ionizing radiation. *J. Biol. Chem.* **277**, 12491–12494 (2002).

Web Figure A. p53 phosphorylation at Thr18, Ser20, Ser33, Ser37 and Ser46 in IMR-90 cells after UV (15J/m$^2$) or infection with H-rasV12.

This addendum supplements data in Fig.1*b* and shows three panels of Western blots:
(A) Shows no phosphorylation at Thr18, Ser20 or Ser37 in IMR-90 cells irradiated with UV (15J/m$^2$) or infected with H-rasV12 vs control. Extracts of A549 cells exposed to UV light served as a positive antibody control.
(B) Time course (4h to 48h) of p53 phosphorylatin at Ser33 and Ser46 in IMR-90 cells after exposure to UV (15J/m$^2$). The data indicate that phosphorylation after UV decreased to basal levels by 48h.
(C) Phosphorylation of p53 at Ser33 and Ser46 in IMR-90 cells at day 1 and day 5 after infection with H-rasV12 or vector and selection with puromycin. The data show that phosphorylation levels remain constant.

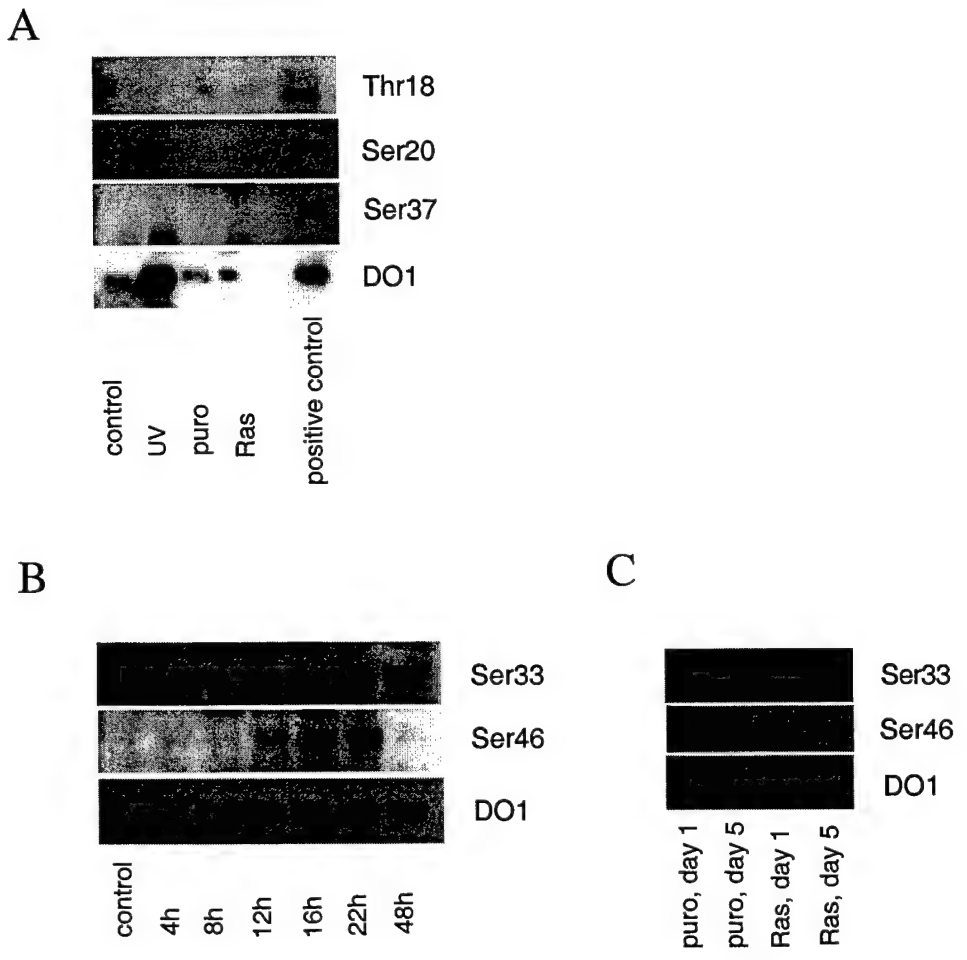

Web Figure D. Activation of p38 MAPK in *Ppm1d*$^{-/-}$ cells.
The activities of Erk, JNK and p38 MAPK in thymocytes from either wildtype or *Ppm1d*$^{-/-}$ mice were assessed using phospho-specific antibodies (designated by "-P") and a Western immunoblot assay. Total protein was assessed with corresponding antibodies that recognize both the phosphorylated and non-phosphorylated proteins. Antibodies were from Santa Cruz ( Erk2 (C-14), JNK (C-17), p38 (C-20)) and Cell Signaling (Erk-P, JNK-P, p38-P, Hsp27-P). Hsp27-P served as an endogenous substrate for p38 MAPK.

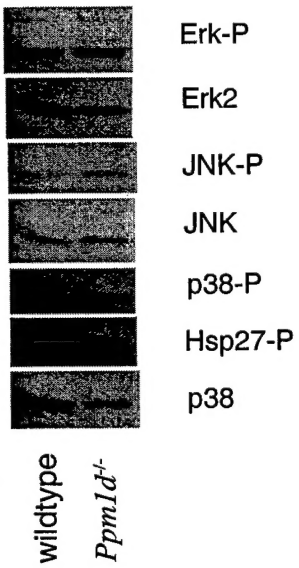

Web Figure C. Role of Wip1 in the p38 MAPK/p53 pathway in regulating tumorigenesis *in vivo*.

(A) Nude mice were injected on the right side with wildtype MEFs infected with E1A+H-rasV12+HPV16-E6-expressing retroviruses or on the right with *Mapk14*$^{-/-}$ MEFs infected with the same retroviruses.

(B) Same as A, but MEFs were injected with Wip1 and then with E1A+Ras expressing retroviruses. Tumor weight data for panels A and B are given in the text.

(C) Mice were injected on the right side with wildtype MEFs infected with E1A+Ras –expressing retroviruses or on the left side with wildtype MEFs infected with E1A+Ras+Wip1-expressing retroviruses.

(D) Same as C, but *Mapk14*$^{-/-}$ MEFs were used instead of wildtype cells.

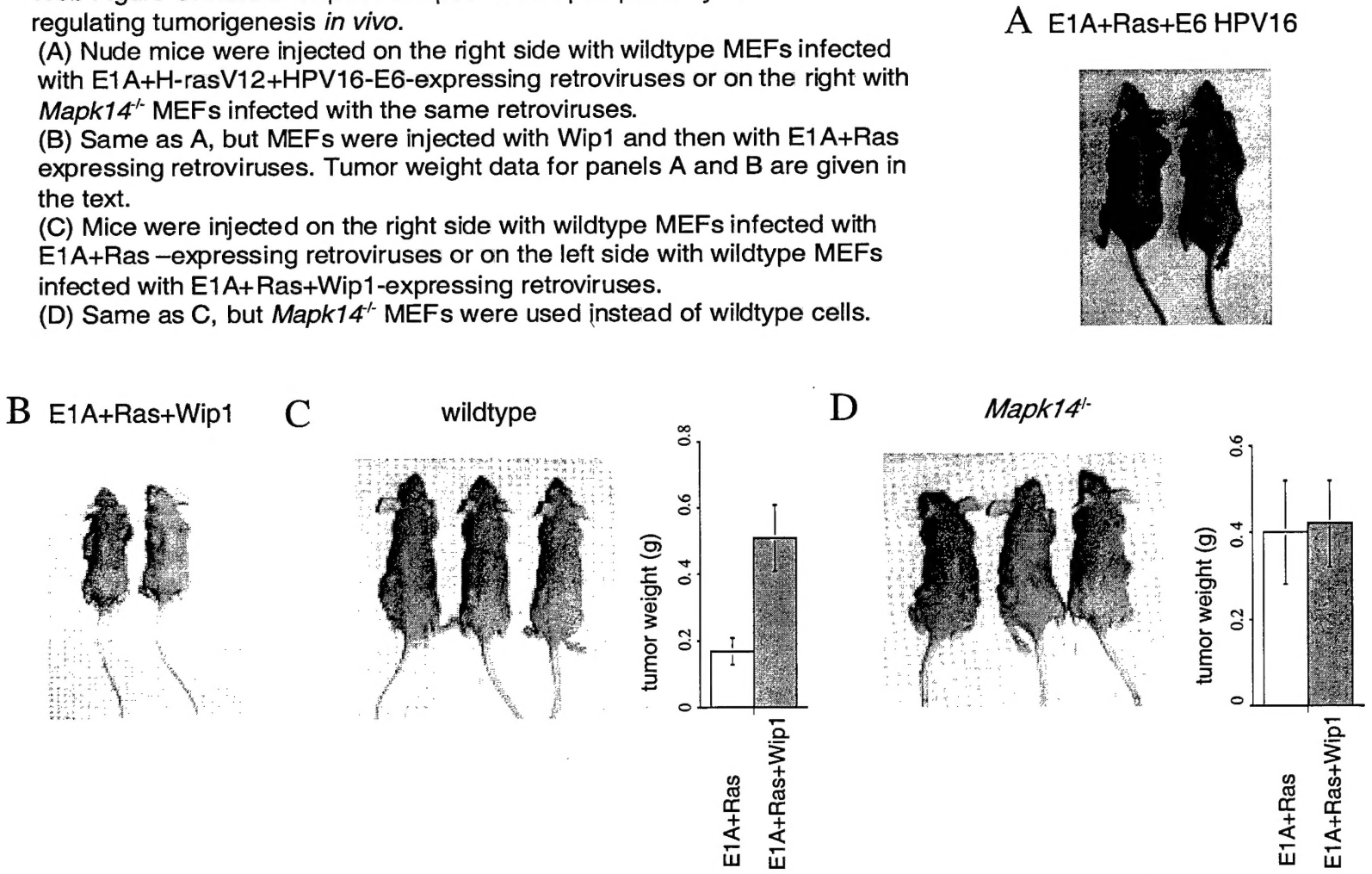

Web Figure B. Wip1 complements H-rasV12 for transformation of wildtype MEFs.

Transformation of wildtype and *Trp53*$^{-/-}$ MEFs was determined after infection with vector (puro), H-rasV12-expressing virus, vector (puro) and Wip1-expressing virus, or H-rasV12- and Wip1-expressing virus.
Cells were seeded in 100 mm plates after 4 days of selection with puromycin, the medium was changed every 3 days during the next 3 weeks, then foci were stained with crystal violet.

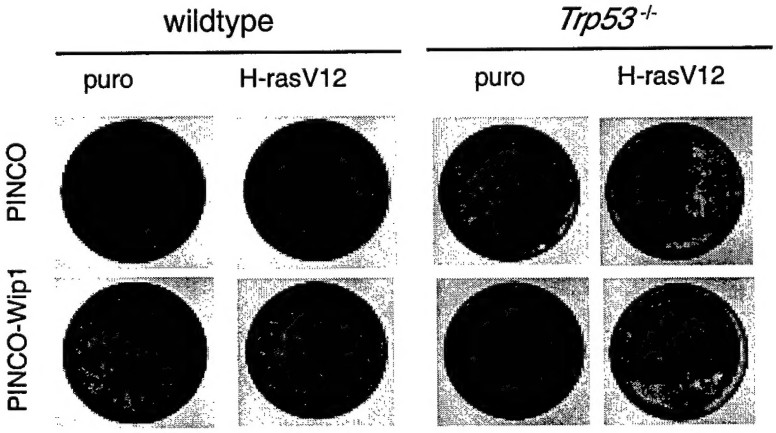

## Web Table A. *PPM1D* mRNA level* in the panel of 64 human tumor cell lines

| cell line | p53 | tissue | Wip1 | cell line | p53 | tissue | Wip1 |
|---|---|---|---|---|---|---|---|
| IMR-90 | wt | 1° epithelial | 1.0 | COLO205 | mut | colon | 0.3 |
| A549 | wt | lung | 0.5 | HCT116 | wt | colon | 1.4 |
| EKVX | mut | lung | 0.9 | HCT15 | mut | colon | 1.6 |
| HOP62 | mut | lung | 1.1 | HT29 | mut | colon | 0.3 |
| HOP92 | mut | lung | 1.3 | KM12 | mut | colon | 0.5 |
| NCI-H226 | mut | lung | 1.0 | SW620 | mut | colon | 1.2 |
| NCI-H23 | mut | lung | 0.7 | HeLa | wt | cervix | 1.1 |
| NCI-H322M | mut | lung | 0.5 | CCRF-CEM | mut | lymph | 1.6 |
| NCI-H460 | wt | lung | 0.5 | HL60 | mut | lymph | 1.3 |
| NCI-H522 | mut | lung | 1.7 | K562 | mut | lymph | 1.6 |
| BT549 | mut | breast | 0.3 | MOLT4 | wt | lymph | 2.3 |
| HS578T | mut | breast | 0.3 | RPMI 8226 | mut | lymph | 1.0 |
| MCF7 | wt | breast | 7.3 | SR | wt | lymph | 1.0 |
| NCI-ADR | mut | breast | 1.5 | TK6 | wt | lymph | 1.4 |
| MDA-MB157 | ? | breast | 1.7 | WTK1 | mut | lymph | 0.7 |
| MDA-MB361 | ? | breast | 4.7 | 786-O | mut | renal | 0.4 |
| MDA-MB231 | mut | breast | 0.8 | A498 | wt | renal | 1.4 |
| MDA-MB436 | ? | breast | 0.6 | CAKI-1 | wt | renal | 2.2 |
| MDA-N | mut | breast | 0.6 | RXF-393 | mut | renal | 0.4 |
| T47D | mut | breast | 0.9 | SN12C | mut | renal | 0.3 |
| Sum52 | ? | breast | 1.5 | TK10 | mut | renal | 1.5 |
| BT474 | mut | breast | 4.8 | UO31 | wt | renal | 1.5 |
| KPL-1 | wt | breast | 9.4 | LOX-IVMI | wt | melanoma | 1.2 |
| SF-268 | mut | cns | 0.7 | M14 | mut | melanoma | 1.1 |
| SF-295 | mut | cns | 1.0 | SK MEL2 | mut | melanoma | 0.9 |
| SF-539 | wt | cns | 0.9 | SK MEL28 | mut | melanoma | 1.1 |
| SNB19 | mut | cns | 1.0 | SK-MEL5 | wt | melanoma | 0.6 |
| IGROV-1 | wt | ovary | 0.8 | UACC-257 | wt | melanoma | 1.6 |
| OVCAR3 | mut | ovary | 1.0 | UACC-62 | wt | melanoma | 0.3 |
| OVCAR4 | wt | ovary | 2.2 | LNCaP | wt | prostate | 1.3 |
| OVCAR5 | mut | ovary | 0.8 | DU-145 | mut | prostate | 1.6 |
| OVCAR8 | mut | ovary | 1.1 | PC3 | mut | prostate | 0.9 |
| SKOV-3 | mut | ovary | 0.8 | | | | |

* *PPM1D* mRNA levels were determined in 64 human tumor cell lines[14] using a dot-blotting procedure; polyU served as a control for relative mRNA content. Values are reported relative to the level in IMR-90 cells, a normal, human, lung-derived, fibroblast cell line that expresses wildtype p53. The p53 status and tissue source of the tumor cell lines is given; wt, wildtype p53; mut, mutant p53; ?, p53 status not known; cns, central nervous system.